JOURNAL OF PROPULSION AND POWER
Vol. 24, No. 1, January–February 2008

Testing a Helicon Double Layer Thruster Immersed in a Space-Simulation Chamber

Michael D. West,* Christine Charles,† and Rod W. Boswell‡
Australian National University, Canberra, Australian Capital Territory 0200, Australia

DOI: 10.2514/1.31414

The Helicon Double Layer Thruster, a new magnetoplasma thruster that accelerates ions to supersonic velocities using a current-free electric double layer, has been tested successfully for the first time inside a space-simulation vacuum chamber. Using a retarding field energy analyzer, the presence of a current-free double layer and the associated ion beam in argon have been confirmed for operating conditions of 0.297 mgs^{-1} of argon, 53.3 mPa gas pressure, 100 W of radio-frequency forward power at 13.56 MHz, and a maximum axial magnetic field of 138 G. The inductively coupled plasma and ion beam formed have been characterized axially, and the measured beam velocity is about 8.7 kms^{-1} for these conditions. The effect of moving the Helicon Double Layer Thruster source tube relative to the magnetic field and radio-frequency antenna is investigated, and the pressure dependence of the double layer is measured from 20 to 275 mPa and compared with a recently developed theoretical model. Ions in the Helicon Double Layer Thruster exhaust are also shown to be nonmagnetized, suggesting that ion detachment has occurred.

Nomenclature

A_p	=	Langmuir probe area, mm^2
B_z	=	axial dc magnetic field, G
c_s	=	Bohm velocity, kms^{-1}
e	=	electron charge, C
I_{beam}	=	retarding field energy analyzer current at ion beam energy, A
I_c	=	retarding field energy analyzer collector current, A
I_{sat}	=	ion saturation current, A
k	=	Boltzmann's constant, JK^{-1}
M	=	mass of the argon ion, kg
n	=	plasma density, cm^{-3}
p	=	pressure, Pa
r_{ge}	=	electron gyroradius, m
r_{gi}	=	ion gyroradius, m
T_e	=	electron temperature, eV
T_i	=	ion temperature, eV
v_{beam}	=	ion beam velocity, kms^{-1}
v_{T_e}	=	electron velocity at given temperature, kms^{-1}
v_{T_i}	=	ion velocity at a given temperature, kms^{-1}
V_{beam}	=	ion beam energy, V
V_{DL}	=	potential drop of the double layer, V
V_d	=	retarding field energy analyzer discriminator voltage, V
V_{local}	=	local plasma potential, V
Z	=	charge state
z	=	axial position, cm
λ	=	effective mean free path, cm
λ_i	=	ion-neutral mean free path, cm
μ	=	ion–proton mass ratio
ω_{ce}	=	electron gyrofrequency, Hz
ω_{ci}	=	ion gyrofrequency, Hz

Received 4 April 2007; revision received 11 October 2007; accepted for publication 12 October 2007.

*Ph.D. Candidate, Space Plasma, Power & Propulsion Group, Research School of Physical Sciences & Engineering; michael.west@anu.edu.au. Student Member AIAA.

†Senior Research Fellow, Space Plasma, Power & Propulsion Group, Research School of Physical Sciences & Engineering.

‡Professor, Space Plasma, Power & Propulsion Group, Research School of Physical Sciences & Engineering.

I. Introduction

CURRENT-FREE electric double layers, which accelerate ions, have been observed in recent years in various laboratory plasma experiments of different shapes and sizes at low pressures (less than 135 mPa) in the presence of a diverging magnetic field [1,2]. All of these experiments consist of a plasma source tube attached to a larger-diameter vacuum chamber and are based on systems used for materials processing (Chi Kung [1] and other helicon reactors [3]) or studies of fundamental plasma and astrophysical phenomena [Waves on Magnetized Beams and Turbulence (WOMBAT) experiment [4], Magnetic Nozzle Experiment (MNX) [5,6], and Hot Helicon Experiment (HELIX) [7]]. If current-free electric double layers are to be used in electric propulsion applications for spacecraft [1,8,9], it is imperative that such a system is tested in a configuration in which the plasma source (and the whole thruster) is immersed inside a space-simulation vacuum chamber. Such a configuration more accurately reflects the proposed application and will provide insights into concerns raised about the operation of this thruster type in space.

These concerns have centered around three interrelated issues:

1) Is the presence of the double layer, and hence the ion beam, dependent upon the physical geometry of the source tube and that of the expansion region? That is, is a double layer formed when the region downstream of the source is infinite, such as when used as a spacecraft thruster?

2) Is the double layer dependent upon the interaction of the downstream plasma and to what extent does it influence the double layer and ion beam properties?

3) Does the plasma detach from the spacecraft to produce thrust? [10].

In this paper, we show the first experimental evidence of a current-free double layer and ion beam formation with the prototype of the Helicon Double Layer Thruster (HDLT) operating inside a large volume space-simulation vacuum chamber.

II. Helicon Double Layer Thruster Concept

The HDLT is a magnetoplasma thruster based upon the recent discovery of a current-free electric double layer in an inductively coupled plasma that is driven by a helicon antenna, expanding in a diverging magnetic field. It is proposed that thrust is produced when ions are ejected by the double layer at supersonic velocities at the thruster exit. The ion beam has a low beam divergence (less than 5 deg for argon and 6 deg for xenon [11]), constant velocity across the thruster radius, and exhaust velocities of up to 15 kms^{-1} [12,13]. These properties lead to a moderately high specific impulse (between 1000 and 1500 s) and a high thrust-vector efficiency [8]. Double

layers have been created in experiments with a variety of gases, including argon, hydrogen [14], oxygen, and xenon[11], the latter being the propellant most commonly used for Hall-effect thrusters and ion engines. Electronegative double layers have also been measured recently [3] in mixtures of Ar/SF_6 in the absence of a magnetic field, but the potential drop of the double layer is less than the electropositive case.

The HDLT is scalable in both size and power, with various experiments worldwide demonstrating ion beam formation in helicon sources of various diameters [4] and operating at various levels of radio-frequency power. The HDLT has no electrodes, accelerating grids, or neutralizer, which limit the operating life of other electric propulsion systems. Erosion of the Pyrex source tube depends upon the impact energy of the argon ions onto the source-tube walls. This is a function of the wall sheath potential, which has been measured and modeled [15] as typically less than 100 eV. The SiO_2 etch rate for argon ions is near zero below 200 eV [16], and so such erosion will be minimal. Without these failure modes, the HDLT is an attractive option for large spacecraft requiring high delta-V and long-duration missions such as interplanetary probes with large science payloads, cargo missions to Mars and the Moon, and long-duration satellite station-keeping in Earth orbit.

III. Experimental Setup

The Helicon Double Layer Thruster, as described recently by Charles et al. [11] consists of a Pyrex source tube, with a closed end of Pyrex, 5-mm wall thickness, 15 cm in diameter, and a length (and hence insulating plasma cavity) of 29 cm. The source tube is mounted inside the HDLT structure, which is made of sandblasted aluminum. The HDLT structure consists of three rectangular panels for thermal radiation, mounted perpendicularly to the axis of the source tube, and two solenoids, the axes of which are mounted parallel to the axis of the source tube. The source tube of the HDLT can be moved axially with respect to the HDLT structure and the solenoids. For the present experiments, the source tube is positioned either in line with the HDLT structure (i.e., the end of the source tube is at $z = 0$ cm) or it extends 3 cm beyond the HDLT structure (i.e., the end of the source tube is at $z = 3$ cm). The solenoids produce a divergent magnetic field with an axial maximum of 138 G at $z = -5$ cm that decreases to a few gauss downstream. A double-saddle field antenna, based on that invented by Boswell [17,18], constructed from copper with a 25-μm silver plating and 18 cm long surrounds the source tube and is attached to the inside of the HDLT structure. The antenna is a few millimeters from the source tube to minimize capacitive coupling and to limit thermal effects. The antenna is not in contact with the source tube, allowing for independent movement of the source tube relative to the antenna and HDLT structure.

The HDLT is installed, as shown in Fig. 1, inside a space-simulation vacuum chamber 1 m in diameter and 1.4 m long. The chamber is manufactured from nonmagnetic stainless steel that is resistant to deformation caused by thermal cycles, high vacuum, and outgassing to simulate the vacuum conditions of low Earth orbit, in which the pressures are typically less than 10^{-4} Pa [19]. The vacuum chamber has a turbomolecular/rotary pumping system that maintains a base pressure less than 1.2×10^{-4} Pa, and the effective pumping speed measured for argon is approximately 330 ls^{-1}. At such pressures, the thermal environment of outer space can be simulated, because the thermal conduction of gases is small, relative to the radiant heat transfer. The gas flow inside the space-simulation chamber is also in the free-molecular-flow regime, in which each gas acts independently of all others present [20]. The chamber pressure is measured using a Granville-Phillips Convectron gauge, a MKS 220CA Baratron gauge and a Granville-Phillips Series 274 ionization gauge tube, which are all located at the downstream end of the vacuum chamber, as shown in Fig. 1. The stated base pressure is measured with the ionization gauge tube and corrected for argon. All other pressure measurements in this work are made with the Baratron gauge, which is gas-species-independent, and so no correction for argon is required.

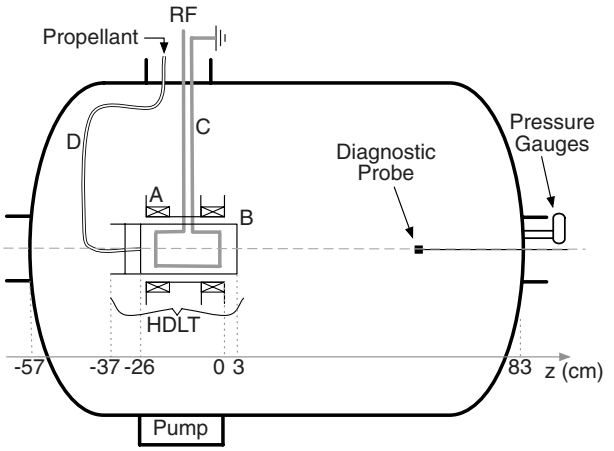

Fig. 1 Schematic of the Helicon Double Layer Thruster mounted inside the space-simulation vaccuum chamber; HDLT consists of structure with two solenoids (A), pyrex source tube (B), shielded copper rods attached to double-saddle field antenna (C), and a nylon propellant line (D).

A flange on the side of the space-simulation vacuum chamber provides feedthrough for the propellant line, power for the solenoids, and radio-frequency (RF) power for the antenna. The propellant (in this case, argon) is injected into the source tube using nylon tubing attached to its closed end, and its flow rate is regulated by a mass flow controller mounted outside the vacuum chamber. The flow controller used is a MKS Type 2160B mass flow controller that has an accuracy of $\pm 1\%$.

A RF matching network/generator on the outside of the vacuum chamber is connected to the antenna of the HDLT by two copper rods enclosed in a copper shield. The matching network is a custom-built π impedance matching network that uses two tunable vacuum capacitors. A Revex W502 standing wave reflected and power meter is used to measure the forward and reflected power. The RF power (13.56 MHz) is maintained at 100 W of forward power to reduce the thermal loading on the HDLT. For similar reasons, the current applied to each solenoid was limited to 3 A to avoid overheating and melting of the solenoid copper wire.

As shown in Fig. 1, the system is divided into the downstream region of the space-simulation vacuum chamber (positive numbers) and the source region of the HDLT (negative numbers). The end of the HDLT source tube is initially at $z = 3$ cm, the maximum of the magnetic field is at $z = -5$ cm, and the maximum magnetic field gradient is at $z = 2$ cm. Figure 2 shows the axial dc magnetic field component B_z for this study as a function of axial position. B_z was measured using a three-axis Bell 640 Hall-effect gaussmeter that has an accuracy of $\pm 0.65\%$. The axial position accuracy of the gaussmeter is ± 5 mm. To highlight the location of the magnetic field relative to the HDLT, a schematic of the HDLT is also shown in Fig. 2.

IV. Diagnostics

To confirm the presence of a current-free double layer and the associated ion beam, the ion energy distribution function (IEDF) and the plasma density are measured as a function of the axial position by a retarding field energy analyzer (RFEA). The RFEA consists of three grids and a collector plate. The plasma particles enter the analyzer through a 2-mm aperture in a 0.1-mm-thick stainless steel orifice plate. The orifice plate is in electrical contact with the analyzer housing, which is connected to the grounded space-simulation vacuum chamber. More details on the RFEA design and construction are outlined by Conway et al. [21] and Charles et al. [22].

The voltages on the grids of the analyzer are set at -90, -18, and -9 V for the repeller grid, secondary grid, and the collector plate, respectively. The discriminator grid is located between the repeller and the secondary grid. The voltage applied to the repeller grid is sufficient to repel most plasma electrons during the IEDF

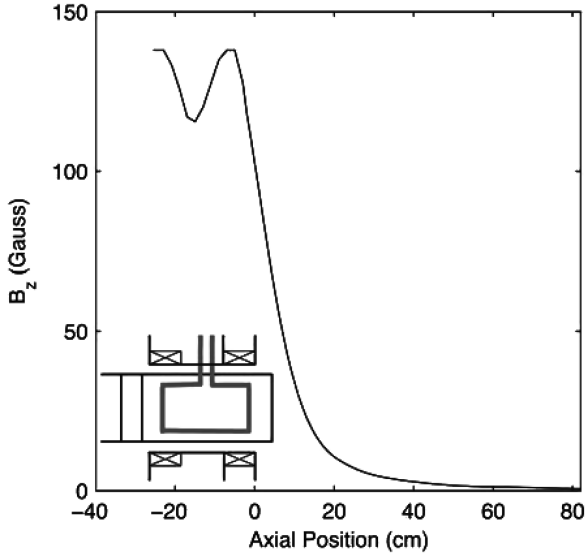

Fig. 2 B_z component of the dc magnetic field along the axis from the inside of the HDLT source to the end of the space-simulation vacuum chamber; the schematic of the HDLT is also shown.

measurements, and the small bias applied to the collector plate ensures that all ions are collected at the collector [21]. The measured current is the sum of the collector current and the secondary grid current, which corresponds to any secondary electrons emitted from the collector plate upon ion impact [23]. To achieve this, the bias of the secondary grid is set to −18 V. The analyzer is used in the ion-collection mode only. The voltage on the discriminator grid is swept from 0 to +100 V, in increments of 0.5 V, with 100 current measurements averaged per increment to produce a time-averaged ion-current-vs-discriminator-voltage (I_c-vs-V_d) curve. These data are collected using a LabView data acquisition system and the results are shown in Figs. 3a and 4a. The measured energy resolution of an RFEA of this construction is better than 1 eV, as determined by Charles et al. [22].

The RFEA is mounted on the centerline of the HDLT and the space-simulation vacuum chamber with the RFEA entrance orifice facing the HDLT exhaust, as shown in Fig. 1. This configuration allows for simultaneous measurements of the local plasma potential V_{local}, ion beam energy V_{beam}, and the plasma density n. A MATLAB program is used to analyze the data obtained and to hence determine these parameters. First, the measured I_c-vs-V_d characteristic is smoothed using a Savitzky–Golay smoothing filter [24]. This filtering method has the advantage of preserving the features of the I_c-vs-V_d characteristic, which are usually flattened by other averaging techniques that use adjacent data points to smooth the data, such as applying a moving average. The IEDF is computed as $-\mathrm{d}I_c/\mathrm{d}V_d$, and so the smoothed I_c-vs-V_d characteristic is then differentiated to obtain the experimental IEDFs, as shown in Figs. 3b and 4b (dashed-dotted line). To enable systematic analysis, the experimental IEDF is fitted with the sum of two independent Gaussian functions. The centers of the Gaussian functions (solid line in Fig. 4b) correspond to V_{local} and V_{beam}, respectively. When only one Gaussian function (solid line in Fig. 3b) can be fitted, its center corresponds to V_{local} only.

To determine the plasma density n using the RFEA, the analyzer was first calibrated using a planar disc Langmuir probe that was 3.97 mm in diameter. The Langmuir probe was mounted on the centerline of the HDLT and space-simulation vacuum chamber and placed inside the HDLT source at $z = 7$ cm. With the Langmuir probe biased at −90 V to be in the ion-collection mode and with a plasma created at a flow rate of 1.49 mgs^{-1}, a pressure of 0.267 Pa, 100 W of forward RF power, and a magnetic field of 138 G, the ion saturation current I_{sat} was measured. This method of calibration, with a higher-density plasma produced at a higher pressure, is commonly employed to calibrate RFEAs [22], and the RFEA does not behave differently at lower pressures [23,25]. $I_c(V_d = 0)$, the total current

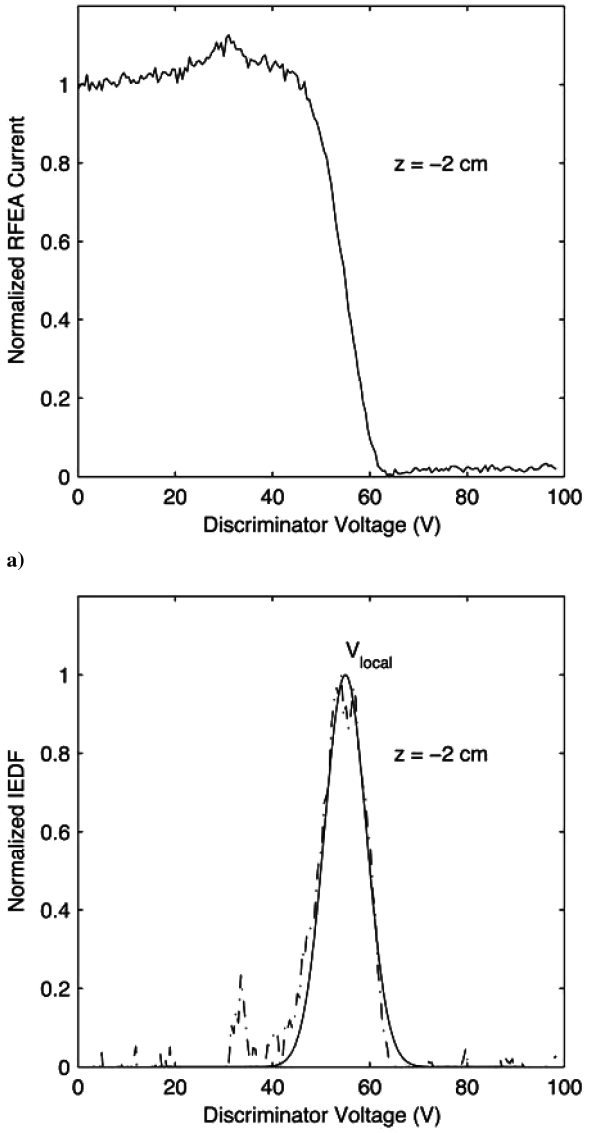

Fig. 3 Measurements with the RFEA placed upstream at $z = -2$ cm: a) raw RFEA current and b) normalized IEDF with raw data (dashed-dotted line) and Gaussian fits (solid line) shown. Discriminator voltages are measured relative to chamber ground.

measured by the RFEA, was then measured under the same conditions at $z = 7$ cm. The RFEA was then calibrated for plasma density measurements using the ion-saturation-current expression:

$$I_{\text{sat}} = 0.6eA_p c_s n \tag{1}$$

where e is the electron charge, A_p is the area of the Langmuir probe, n is the plasma density, and $c_s = (kT_e/M)^{1/2}$, where k is Boltzmann's constant, T_e is the electron temperature, and M is the argon ion mass.

The Langmuir probe was also used to measure the electron temperature downstream, and T_e was found to be about 5.2 eV and is assumed to be constant along the z axis downstream. T_e was deduced from the I–V characteristics of the Langmuir probe using the usual I–V curve processing methods (i.e., the gradient of a linear fit of the natural logarithm of the electron current).

V. Experimental Results and Discussion

A. Plasma and Ion Beam Characterization

The characterization of the plasma and ion beam created by the HDLT was undertaken with a propellant flow rate of 0.297 mgs^{-1} of argon, resulting in a pressure of 53.3 mPa. This pressure is similar to that used in past experiments, in which current-free double layers

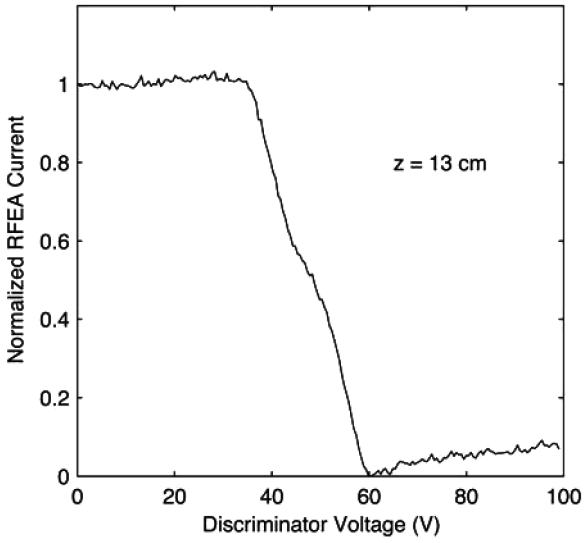

Fig. 4 Measurements with the RFEA placed downstream at $z = 13$ cm: a) raw RFEA current and b) normalized IEDF with raw data (dashed-dotted line) and Gaussian fits (solid line) shown. Discriminator voltages are measured relative to chamber ground.

have been found, and is within the pressure range predicted by a model recently developed for current-free double layer formation [15,26]. The HDLT source tube was extended 3 cm beyond the HDLT structure: that is, where $z = 3$ cm is the end of the source tube, because in previous experiments when the HDLT was attached to the Chi Kung vacuum chamber, the source tube also extended 3 cm beyond the HDLT structure. All measurements are conducted with the plasma in a steady-state equilibrium. Figure 3 shows the I_c-vs-V_d characteristic and the IEDF obtained when the RFEA is located upstream, 5 cm inside the HDLT source at $z = -2$ cm. The accuracy in the position of the RFEA is ± 2 mm. No ion beam is detected upstream inside the HDLT source, because only one Gaussian function can be fitted to the experimental data. V_{local} corresponds to the center of this Gaussian function and at this position is 55 V, relative to chamber ground. This result corresponds well with measurements made at a similar pressure in Chi Kung with a different RFEA probe calibrated with a Langmuir probe [27].

With the RFEA located 10 cm downstream at $z = 13$ cm, the I_c-vs-V_d characteristic and the IEDF shown in Fig. 4 are obtained. This position is chosen because past RFEA measurements in the Chi Kung experiment have been made at a similar distance from the exit of the source tube. In Fig. 4a, the small increase in collector current in

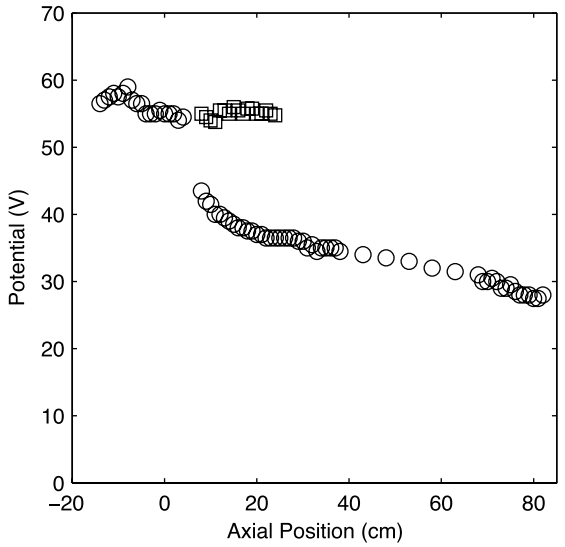

Fig. 5 Local plasma potential V_{local} (open circles) and ion beam potential V_{beam} (open squares) as a functions of axial position. The experimental uncertainty on the potential is ± 2 V.

the region beyond 60 V in the I_c-vs-V_d characteristic is a result of secondary electron emission from the RFEA collector plate, which is a common occurrence with RFEAs [23] and does not affect the experimental IEDFs produced. The IEDF in Fig. 4b shows a clear ion beam, represented by the second peak of the IEDF, which is centered at 55.5 V. The center of the first peak is the local plasma potential at the probe location and is $V_{\text{local}} = 39.5$ V. Because RFEA discriminator voltages are measured relative to the chamber ground, the directed beam energy shown in Fig. 4b does not indicate a directed beam energy of 55.5 V, but rather a beam energy of 16 V on top of a plasma potential of 39.5 V. The resultant direct beam energy will be discussed further in later sections. Both V_{local} and V_{beam} measured downstream are in good agreement with that measured in Chi Kung at a similar pressure with a calibrated RFEA [27]. The local plasma potential inside the source, $V_{\text{local}} = 55$ V, corresponds well, within the limits of the experimental error (± 2 V), with the ion beam energy downstream.

Figure 5 shows the potentials of the local plasma and the ion beam as a function of axial position for the operating conditions described previously. The ion beam is detectable with the RFEA up to 21 cm downstream from the exit of the HDLT source at position $z = 24$ cm. Ion-neutral charge-exchange collisions are the main process involved in damping the ion beam. For thermal ions in low-pressure plasmas, with ion temperatures around 0.1 eV, the ion-neutral mean free path for argon (in centimeters) is $\lambda_i = (2.475p)^{-1}$, where p is the pressure in Pa. A correction factor for the mean free path must be applied because the charge-exchange cross section is velocity-dependent [28]. For a 15-eV beam, the estimated effective mean free path is $\lambda = \lambda_i/0.7$ [15]. At 53.3 mPa, $\lambda \sim 10$ cm, and therefore the ion beam could be measured for approximately two mean free paths before damping by ion-neutral charge-exchange collisions merges the signal into the background.

The density profile is another important plasma characteristic and can be used to compare the results for this experiment with other investigations. The total current measured by the calibrated RFEA, $I_c(V_d = 0)$, was used to determine the density profile for the conditions described previously (0.297 mgs^{-1}, 53.3 mPa, 100 W, and 138 G). Figure 6 shows the plasma density n as a function of axial position. The plasma density upstream decreases from a maximum at $z = -13$ cm of $\sim 5.0 \times 10^{10}$ to $\sim 2.5 \times 10^{10}$ cm^{-3} at the end of the HDLT source tube ($z = 3$ cm). The plasma density in the downstream region is reasonably constant around $\sim 1.0 \times 10^{10}$ cm^{-3} in the region from $z = 12$ to 32 cm. This is also the region in which the ion beam is detected with the RFEA. As the plasma diffuses downstream, the plasma density decreases as a result of diffusion until reaching the back of the space-simulation chamber ($z = 83$ cm), where the density is $\sim 2.0 \times 10^9$ cm^{-3}.

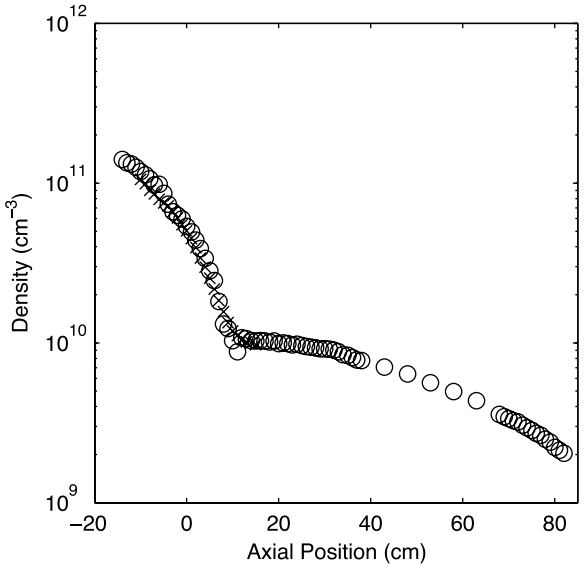

Fig. 6 Plasma density n as a function of axial position; standard conditions described in Sec. III (open circles) and with HDLT source tube retracted 3 cm, as described later in Sec. V.C (crosses). The experimental uncertainty is less than 10%.

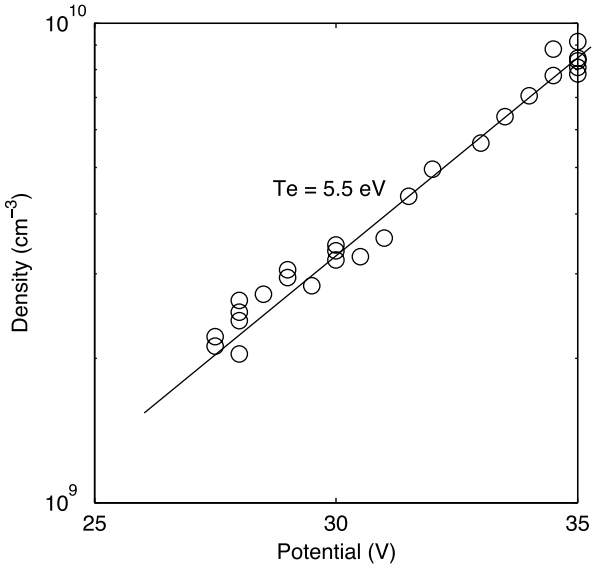

Fig. 7 Plasma density n as a function of local plasma potential V_{local} downstream. The experimental uncertainty is less than 10%.

The density profile measured with the RFEA and shown in Fig. 6 is consistent with the current-free double layers measured via the Langmuir probe and other diagnostics in previous experiments with "standard" configurations such as Chi Kung [1]. The densities on both sides of the double layer and the general shape of the plasma density profile conforms with the theoretical model for low-pressure current-free double layers developed recently [15,26]. In this experiment, the plasma density profile is measuring both the thermal and beam ions because the RFEA is facing the HDLT source. The experiments undertaken in Chi Kung [1] use an axial RFEA facing radially so that only the thermal ions are measured. In that case, a density discontinuity is revealed at the location of the double layer. Nonetheless, the density profile obtained here is consistent with that found in Chi Kung if the RFEA was facing the source and both thermal and beam ions were measured.

When using the Langmuir probe as described in Sec. IV, the exhaust region of the HDLT was investigated between $z = 8$ and 18 cm for the conditions described previously (0.297 mgs^{-1}, 53.3 mPa, 100 W, and 138 G). The electron temperature was measured across this region to be 5.2 ± 0.5 eV. In addition, the Boltzmann relation,

$$n_1 = n_2 \exp[(V_{\text{local1}} - V_{\text{local2}})/T_e] \tag{2}$$

can be used to deduce the electron temperature and demonstrate that there is a Boltzmann expansion downstream with a constant electron temperature [25,29–31]. Parameters n_1, V_{local1} and n_2, V_{local2} are the plasma density and local plasma potential measured with the RFEA in two locations. The electron temperature is found by rearranging Eq. (2) such that

$$T_e = \frac{V_{\text{local1}} - V_{\text{local2}}}{\ell n(n_1/n_2)} \tag{3}$$

Figure 7 shows the a logarithmic plot of the plasma density measured with the RFEA versus the local plasma potential measured with the RFEA in the region downstream of the source for the conditions described previously (0.297 mgs^{-1}, 53.3 mPa, 100 W, and 138 G). The data in this region fit very well to a straight line, and the slope yields an electron temperature of 5.5 eV [from Eq. (3)]. This result is in good agreement with the temperature deduced from the Langmuir probe measurements described earlier and suggests that downstream of the HDLT source, the plasma follows a Boltzmann expansion [25,30,31].

From Fig. 5, the local plasma potential downstream of the source drops off at a rate of approximately 13 Vm^{-1} until it reaches the back of the space-simulation vacuum chamber, in which the plasma potential measured with the RFEA is ~28 V. Using the Langmuir probe, the plasma potential measured at the back wall ($z = 83$ cm) ~26 V. In both cases, the measured potential is about $5T_e$. These results confirm that the diagnostics are in good agreement and show that the back wall is in fact grounded.

B. Double Layer Characteristics

We have found experimentally that in this configuration, it is difficult to determine the precise location of the potential discontinuity associated with the double layer using an RFEA facing the HDLT source. The use of an axial RFEA facing radially may provide better information on the double layer position, because the RFEA would only measure the thermal ion population at the local plasma potential and not the ion beam population at the higher potential, because the RFEA orifice would not be facing the ion beam [1,15]. This will be pursued in future studies. However, it is clear from the IEDFs obtained, such as that in Fig. 4b, that an ion beam is present downstream. From Fig. 5, it is also clear that the double layer is located somewhere in the region between $z = 1$ and 5 cm. This region is beyond the location of the magnetic field maximum ($z = -5$ cm) but in the region of the maximum of the magnetic field gradient ($z = 2$ cm). In measurements made in WOMBAT [4], Chi Kung [1], and another helicon reactor [3], the position of the double layer is in the vicinity of the location of the maximum of the magnetic field gradient.

The potential drop of the double layer V_{DL}, which equals $V_{\text{beam}} - V_{\text{local}}$, was found to be 16 V when measured with the probe 10 cm from the exit of the HDLT source ($z = 13$ cm). This position was chosen because past measurements of the potential drop of the double layer in the Chi Kung experiment have been made at a similar distance from the exit of the source tube. This result is very similar with that measured in the Chi Kung experiment, on which the HDLT is based, at 53.3 mPa in argon [27] and that observed in other recent investigations [3]. The velocity of the ions in the beam formed by the potential drop V_{DL} can be calculated using

$$v_{\text{beam}} = \sqrt{\frac{2e(V_{\text{beam}} - V_{\text{local}})}{M}} = \sqrt{\frac{2eV_{\text{DL}}}{M}} \tag{4}$$

where e is the electron charge and M is the argon ion mass. In this case, the pressure is 53.3 mPa, $V_{\text{DL}} = 16$ V, and v_{beam} equals ~8.7 kms^{-1}.

Meige et al. [32] found that extending the location of the grounded right wall downstream to 50 cm from the double layer in a particle-in-cell simulation did not influence the potential profile or significantly alter the source plasma potential or the potential drop of the double

layer. In this configuration, in which the grounded wall is 80 cm distant, no significant changes are observed, either. This result suggests that a current-free double layer and ion beam can be formed when the grounded wall is removed completely and the expansion region is infinite, as would be the case when the HDLT is operated in space. This finding is the major conclusion of this paper.

C. Magnetic and Geometric Expansion

To investigate the effect of the position of the source tube, relative to the magnetic field, on the properties of the ion beam and double layer, the HDLT source tube was retracted 3 cm. Hence, the source tube was moved relative to both the structure and the antenna such that the open end of the source is in line with the HDLT structure at $z = 0$ cm. For the same conditions described previously (0.297 mgs^{-1}, 53.3 mPa, 100 W, and 138 G), the RFEA was used to measure V_{DL}, the potential drop of the double layer, at a position 13 cm from the end of the HDLT structure ($z = 13$ cm). This position is 11 cm from the maximum gradient of the magnetic field. Before retracting the HDLT source $V_{DL} = 16$ V, as outlined earlier, and with the source tube retracted 3 cm, $V_{DL} = 15.5$ V. Hence, no appreciable difference in the potential drop of the double layer, and hence the acceleration received by the ions, results from moving the HDLT source tube relative to the magnetic field and the antenna.

The RFEA was also used to determine the density as a function of axial position with the HDLT source tube retracted 3 cm, allowing the effect on the density profile of moving the source tube relative to the magnetic field and antenna to be investigated. Inferences about the effect on the position of the double layer can also be made. Plasma density measurements were made between $z = -10$ and 15 cm for the same conditions described previously (0.297 mgs^{-1}, 53.3 mPa, 100 W, and 138 G) using the RFEA. Figure 6 shows the density profile obtained (stars) with the HDLT source tube retracted 3 cm. When compared with the density profile obtained when the source tube is extended 3 cm beyond the HDLT structure (open circles in Fig. 6), it is clear that the density profile does not change as a result of moving the source tube relative to the magnetic field and the HDLT structure and antenna.

These two results show that the magnitude of the potential drop caused by the double layer is not dependent upon the physical expansion represented by the end of the source tube and that moving the source tube does not adversely affect the formation of the ion beam nor the formation or position of the double layer. When coupled with the conclusion of Sutherland et al. [4] that the position of the double layer is invariant to changes in the position of the magnetic field relative to the physical expansion at the end of the source tube, these results confirm that the double layer is more dependent upon the magnetic field configuration than the physical configuration of the source and the downstream region. This finding is an important conclusion if the HDLT is to be used in spacecraft electric propulsion applications.

D. Pressure Dependence

The HDLT source tube was returned to its original position such that it extends 3 cm beyond the HDLT structure. With the RFEA positioned 10 cm from the exit of the HDLT source tube (at $z = 13$ cm), an experimental study of V_{DL} versus pressure was undertaken. The results are shown in Fig. 8 along with experimental and theoretical data for the Chi Kung experiment [15,26]. The theoretical model was developed recently by Lieberman and Charles [15,26] for the formation of a low-pressure current-free double layer inside an upstream insulating source chamber connected to a larger-diameter vacuum chamber downstream.

In this case (i.e., when the HDLT is immersed inside the space-simulation vacuum chamber), V_{DL} increases rapidly as the pressure is decreased, disappearing at a pressure of 20 mPa, slightly lower than that observed for the Chi Kung experiment. In this experiment, at this pressure, the propellant flow rate is very low, less than 0.1 mgs^{-1}, and so it is not possible to produce a plasma discharge. It is acknowledged that this operating pressure is higher than the operating pressures in orbit, and so studies in a much larger space-simulation vacuum chamber, in which high propellant flow rates are possible while maintaining operating pressures less than 1 mPa, would be beneficial. It is, however, worth noting that Charles et al. [11] have measured a current-free double layer in Chi Kung using xenon at a pressure of 5 mPa. For larger geometries with an inherent and known axial pressure gradient such as the MNX device, which is capable of maintaining pressures in the downstream vacuum chamber below 2 mPa during operation, Cohen et al. [5] and Sun et al. [33] report the formation of current-free double layers.

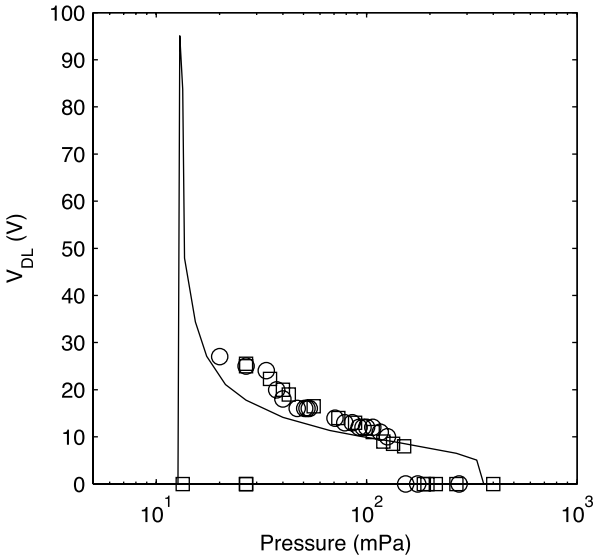

Fig. 8 Double layer strength V_{DL} versus pressure: HDLT immersed in space-simulation vacuum chamber (open circles); results for HDLT attached to Chi Kung vacuum chamber (open squares) and theory (solid line) are from Lieberman and Charles [15,26]. The experimental uncertainty on the potential is ±2 V.

In this experiment, the double layer also disappears at pressures above 133.3 mPa. Past experiments suggest that this occurs when the mean free path becomes much smaller than the source-tube diameter [15]. This result is consistent with the Chi Kung experiment and other recent studies [3].

This agreement suggests that the properties of the double layer and ion beam are consistent with the current-free double layers observed previously in experiments with standard configurations. Therefore, the results from these previous studies may be applied directly to the optimization of the HDLT for space applications.

Furthermore, at 20 mPa, $V_{DL} = 27$ V, which results [using Eq. (4)] in a beam velocity of approximately 11.4 kms^{-1}. This increase in the beam velocity at lower pressures translates into an increase in the specific impulse and demonstrates that the HDLT specific impulse is scalable, an attractive feature for long-duration missions, in which varying levels of thrust and specific impulses may be required.

E. Ion Detachment from the HDLT

Magnetoplasma propulsion systems, such as the HDLT, generate thrust by ejecting a directed flow of magnetized plasma using a magnetic nozzle. The ejected plasma must break free from the spacecraft and the magnetic field lines, which close on the vehicle, to produce a net thrust. If the charged particles attach to the magnetic field lines, they also exhibit a high beam divergence that reduces the thrust efficiency. Conversely, if the beam velocity field has no divergence (i.e., is not influenced by the downstream magnetic field), thrust is generated at maximum efficiency. Several criteria for plasma detachment have been proposed by previous studies. Arefiev and Breizman [34] have proposed a magnetohydrodynamic scenario for plasma detachment in which the magnetic nozzle accelerates the plasma flow to super-Alfvenic velocities and the plasma detaches from the spacecraft together with the field lines, which become stretched along the flow, in a fashion similar to that observed in solar flares and stellar jets. In this scenario, detachment takes place after

the energy density of the expanding magnetic field drops below the kinetic energy density of the plasma.

Alternatively, Gesto et al. [8] have developed a geometric approach to analyzing the magnetic detachment of an ion beam produced by the HDLT, in which detachment occurs if the curvature of the ion motion within the magnetic field approaches zero. Therefore, the detachment point is defined as the point of maximum curvature, and beyond that point, the centrifugal force provided by the magnetic field asymptotes to zero and the gyroradii of the ions become larger than the scales of the experiment. This approach focuses only on the ions in the HDLT exhaust and neglects the effects of ambipolar electric fields generated by the faster transport of electrons along the magnetic field lines downstream. This approach is also supported by experimental evidence that shows that the ion beam formed downstream of current-free electric double layers has a very low divergence [11] and that the ion beam is well-neutralized by sufficient energetic electrons that overcome the potential barrier of the double layer [35]. This last result suggests that a transport mechanism, as yet unidentified, exists that allows the electrons to follow the ions.

Radial measurements of the ion beam, and hence a determination of the beam divergence, with the HDLT immersed in the space-simulation chamber are not possible at this time because of limited access for diagnostics, but will be pursed in future studies. Despite this, some conclusions can be made about the detachment of ions from the HDLT exhaust. Figure 9 shows I_{beam}, the current collected by the RFEA at the discriminator voltage that corresponds to the beam energy, versus the axial position downstream of the HDLT source. The gyroradius for both electrons and ions is also included for the magnetic field present downstream on a logarithmic scale. The gyroradius for electrons, r_{ge}, is found using

$$r_{\text{ge}} = \frac{v_{T_e}}{\omega_{\text{ce}}} = 2.38\,\frac{\sqrt{T_e}}{B_z} \tag{5}$$

where v_{T_e} is the velocity of the electrons at a particular electron temperature, ω_{ce} is the gyrofrequency of the electrons, T_e is the electron temperature in eV (which is assumed to be constant at 5.2 eV), and B_z is the axial magnetic field in gauss. The gyroradius for ions, r_{gi}, is determined using

$$r_{\text{gi}} = \frac{v_{T_i}}{\omega_{\text{ci}}} = 102\,\frac{\sqrt{\mu}}{Z}\,\frac{\sqrt{T_i}}{B_z} \tag{6}$$

where v_{T_i} is the velocity of the ions at a particular ion temperature, ω_{ci} is the gyrofrequency of the ions, μ is the ratio of the ion mass to proton mass (which is 40 for argon), Z is the charge state (which is 1 for Ar^+), T_i is the ion temperature in eV (which is assumed to be 0.2 eV), and B_z is the axial magnetic field in gauss.

It is clear from Fig. 9 that I_{beam}, which is essentially a measure of the ion flux, decreases downstream as a result of collisions, as expected. When the ion beam is first discernible at $z = 8$ cm, the electron gyroradius is 0.18 cm and the ion gyroradius is 8 cm. At $z = 24$ cm, when the ion beam is still detectable, the electron gyroradius is 0.6 cm and the ion gyroradius is 40 cm. At the back wall of the space-simulation vacuum chamber ($z = 83$ cm), the electron and ion gyroradius are 10 and 500 cm, respectively. For reference, the radius of the HDLT source and the space-simulation vacuum chamber are 7.5 and 50 cm, respectively.

Because the acceleration of the double layer is parallel to the magnetic field and the magnetic field is reasonably low (maximum of 138 G), the gyromotion of the ions is not pronounced and their velocity appears to remain axial. Also, the values of the gyroradius approach the scales of the experiment in the region in which the ion beam is detected, which suggests that the ion beam is not magnetized and no longer under the influence of the centrifugal force generated by the magnetic field. Spatially resolved measurements of a supersonic Ar^+ beam downstream of a current-free double layer by Charles [13] using a moveable RFEA in the Chi Kung experiment reached a similar conclusion. When coupled with the work of Gesto et al. [8], these results suggest that the ion beam formed by the HDLT does detach from the magnetic field lines and will produce thrust when operating in space. Further work is required to confirm this conclusion and to determine the beam divergence and thrust efficiency.

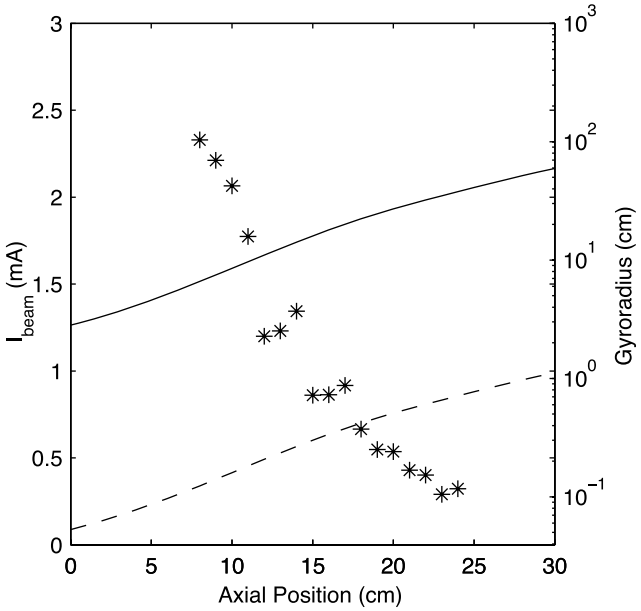

Fig. 9 Current collected at ion beam energy I_{beam} as a function of axial position downstream of the HDLT source (stars); gyroradius for ions (solid line) and electrons (dashed line) under the magnetic field conditions present. The experimental uncertainty is less than 20%.

VI. Conclusions

This study has demonstrated that an ion beam is formed as a result of a current-free electric double layer when the Helicon Double Layer Thruster is immersed in a space-simulation chamber. The beam was detected up to 21 cm downstream and accelerates argon ions to velocities of $\sim$8.7 kms^{-1} at 53.3 mPa and as high as $\sim$11.4 kms^{-1} at 20 mPa. We have shown that the double layer is present in the region between 1 and 5 cm from the exit of the HDLT source and that its potential and density profiles are consistent with experiments in various other configurations. The double layer potential is shown to vary with the pressure in a fashion that is consistent with previous studies and a proposed model for current-free double layer formation. These results provide strong evidence that a double layer can be created independently of the physically expanding geometry of the experiment and the presence of a grounded wall downstream: that is, in a configuration more appropriate to the application of the HDLT as a spacecraft electric propulsion system. In addition, because the properties of the double layer and ion beam are shown to be consistent with current-free double layers in standard configurations, the results from previous studies may also be applied directly to the optimization of the HDLT for space applications.

We have shown, by retracting the HDLT source tube 3 cm, that the magnitude of the double layer potential drop is not changed by moving the source tube relative to the magnetic field and the HDLT structure and antenna. The density profile, and hence the position of the double layer, is also not affected by moving the source tube. Issues associated with plasma detachment and the effect upon thrust generation have been discussed and the gyroradius of the ion beam detected downstream has been determined. The ion gyroradius is shown to approach the radius of the space-simulation chamber, demonstrating that the ions downstream are no longer under the influence of the magnetic field and have detached, and hence the HDLT will produce a net thrust when operating in space.

Acknowledgments

The initial development of the Helicon Double Layer Thruster prototype and the earlier testing phase at the European Space

Research and Technology Centre (ESTEC) in the Netherlands was supported by the International Science Linkages program established under the Australian Government's innovation statement Backing Australia's Ability. The authors wish to thank P. Alexander for his technical assistance on this project.

References

[1] Charles, C., and Boswell, R. W., "Current-Free Double Layer Formation in a High-Density Helicon Discharge," *Applied Physics Letters*, Vol. 82, No. 9, Jan. 2003, pp. 1356–1358. doi:10.1063/1.1557319

[2] Charles, C., "A Review of Recent Laboratory Double Layer Experiments," *Plasma Sources Science and Technology* , Vol. 16, No. 4, 2007, pp. R1–R25. doi:10.1088/0963-0252/16/4/R01

[3] Plihon, N., Chabert, P., and Corr, C. S., "Experiment Investigation of the Double Layers in Expanding Plasmas," *Physics of Plasmas*, Vol. 14, No. 013506, 2007, pp. 1–16. doi:10.1063/1.2424429

[4] Sutherland, O., Charles, C., Plihon, N., and Boswell, R. W., "Experimental Evidence of a Double Layer in a Large Volume Helicon Reactor," *Physical Review Letters*, Vol. 95, No. 205002, Nov. 2005, pp. 1–4. doi:10.1103/PhysRevLett.95.205002

[5] Cohen, S. A., Siefert, N. S., Stange, S., Bolvin, R. F., Scime, E. E., and Levinton, F. M., "Ion Acceleration in Plasmas Emerging from a Helicon-Heated Magnetic-Mirror Device," *Physics of Plasmas*, Vol. 10, No. 6, June 2003, pp. 2593–2598. doi:10.1063/1.1568342

[6] Cohen, S. A., Sun, X., Ferraro, N. M., Scime, E. E., Miah, M., Stange, S., Siefert, N., and Bolvin, R. F., "On Collisionless Ion and Electron Populations in the Magnetic Nozzle Experiment (MNX)," *IEEE Transactions on Plasma Science*, Vol. 34, No. 3, 2006, pp. 792–803. doi:10.1109/TPS.2006.875846

[7] Sun, X., Keese, A. M., Biloiu, C., Scime, E. E., Meige, A., Charles, C., and Boswell, R. W., "Observations of Ion-Beam Formation in a Current-Free Double Layer," *Physical Review Letters*, Vol. 95, No. 025004, July 2005, pp. 1–4. doi:10.1103/PhysRevLett.95.025004

[8] Gesto, F. N., Blackwell, B. D., Charles, C., and Boswell, R. W., "Ion Detachment in the Helicon Double-Layer Thruster Exhaust Beam," *Journal of Propulsion and Power*, Vol. 22, No. 1, 2006, pp. 24–30.

[9] Fruchtman, A., "Electric Field in a Double Layer and the Imparted Momentum," *Physical Review Letters*, Vol. 96, No. 065002, Feb. 2006, pp. 1–4. doi:10.1103/PhysRevLett.96.065002

[10] Hooper, E. B., "Plasma Detachment from a Magnetic Nozzle," *Journal of Propulsion and Power*, Vol. 9, No. 5, 1993, pp. 757–763.

[11] Charles, C., Boswell, R. W., and Lieberman, M. A., "Xenon Ion Beam Characterization in a Helicon Double Layer Thruster," *Applied Physics Letters*, Vol. 89, No. 261503, Dec. 2006, pp. 1–3. doi:10.1063/1.2426881

[12] Charles, C., and Boswell, R. W., "Laboratory Evidence of a Supersonic Ion Beam Generated by a Current-Free 'Helicon' Double-Layer," *Physics of Plasmas*, Vol. 11, No. 4, Jan. 2004, pp. 1706–1714. doi:10.1063/1.1652058

[13] Charles, C., "Spatially Resolved Energy Analyzer Measurements of an Ion Beam on the Low Potential Side of a Current-Free Double Layer," *IEEE Transactions on Plasma Science*, Vol. 33, No. 2, Apr. 2005, pp. 336–337. doi:10.1109/TPS.2005.844958

[14] Charles, C., "Hydrogen Ion Beam Generated by a Current-Free Electric Double Layer in a Helicon Plasma," *Applied Physics Letters*, Vol. 84, No. 3, 2004, pp. 332–334. doi:10.1063/1.1643548

[15] Lieberman, M. A., Charles, C., and Boswell, R. W., "A Theory for Formation of a Low Pressure, Current-Free Double Layer," *Journal of Physics D: Applied Physics*, Vol. 39, No. 15, 2006, pp. 3294–3304. doi:10.1088/0022-3727/39/15/011

[16] Harper, J. M. E., Cuomo, J. J., Leary, P. A., Summa, G. M., Kaufman, H. R., and Bresnock, F. J., "Low Energy Ion Beam Etching," *Journal of the Electrochemical Society*, Vol. 128, No. 5, 1981, pp. 1077–1083. doi:10.1149/1.2127554

[17] Boswell, R. W., "Plasma Production Using a Standing Helicon Wave," *Physics Letters A*, Vol. 33, No. 7, 1970, pp. 457–458. doi:10.1016/0375-9601(70)90606-7

[18] Boswell, R. W., "Very Efficient Plasma Generation by Whistler Waves Near the Lower Hybrid Frequency," *Plasma Physics and Controlled Fusion*, Vol. 26, No. 10, 1984, pp. 1147–1162. doi:10.1088/0741-3335/26/10/001

[19] Tribble, A. C., *The Space Environment: Implications for Spacecraft Design*, Princeton Univ. Press, Princeton, NJ, 2003.

[20] Holkeboer, D. H., Jones, D. W., Pagano, F., and Santeler, D. J., *Vacuum Technology and Space Simulation*, American Vacuum Society Classics of Vacuum Science and Technology, American Inst. of Physics, New York, 1967.

[21] Conway, G. D., Perry, A. J., and Boswell, R. W., "Evolution of Ion and Electron Energy Distributions in Pulsed Plasma Discharges," *Plasma Sources Science and Technology* , Vol. 7, No. 3, 1998, pp. 337–347. doi:10.1088/0963-0252/7/3/012

[22] Charles, C., Degeling, A. W., Sheridan, T. E., Harris, J. H., Lieberman, M. A., and Boswell, R. W., "Absolute Measurements and Modelling of Radio Frequency Electric Fields Using a Retarding Field Energy Analyzer," *Physics of Plasmas*, Vol. 7, No. 12, 2000, pp. 5232–5241. doi:10.1063/1.1322557

[23] Bohm, C., and Perrin, J., "Retarding-Field Energy Analyzer for Measurements of Ion Energy Distributions and Secondary Emission Coefficients in Low-Pressure Radio Frequency Discharges," *Review of Scientific Instruments*, Vol. 64, No. 1, 1993, pp. 31–44. doi:10.1063/1.1144398

[24] Savitzky, A., and Golay, M. J. E., "Smoothing and Differentiation of Data by Simplified Least Squares Procedures," *Analytical Chemistry*, Vol. 36, No. 8, 1964, pp. 1627–1639. doi:10.1021/ac60214a047

[25] Charles, C., Boswell, R. W., and Porteous, R. K., "Measurement and Modeling of Ion Energy Distribution Functions in a Low Pressure Argon Plasma Diffusing from a 13.56 MHz Helicon Source," *Journal of Vacuum Science and Technology*, Vol. 10, No. 2, 1992, pp. 398–403. doi:10.1116/1.578063

[26] Lieberman, M. A., and Charles, C., "Theory for Formation of a Low-Pressure, Current-Free Double Layer," *Physical Review Letters*, Vol. 97, No. 045003, July 2006, pp. 1–4. doi:10.1103/PhysRevLett.97.045003

[27] Charles, C., "High Source Potential Upstream of a Current-Free Electric Double Layer," *Physics of Plasmas*, Vol. 12, No. 044508, 2005, pp. 1–4. doi:10.1063/1.1883182

[28] Lieberman, M. A., and Litchtenberg, A. J., *Principles of Plasma Discharges and Materials Processing*, 2nd ed., Wiley-Interscience, New York, 2005.

[29] Chan, C., Hershkowitz, N., and Lonngren, K. E., "Electron Temperature Differences and Double Layers," *Physics of Fluids*, Vol. 26, No. 6, 1983, pp. 1587–1595. doi:10.1063/1.864294

[30] Charles, C., Boswell, R. W., Bouchoule, A., Laure, C., and Ranson, P., "Plasma Diffusion from a Low Pressure Radio Frequency Source," *Journal of Vacuum Science and Technology A (Vacuum, Surfaces, and Films)*, Vol. 9, No. 3, 1991, pp. 661–663. doi:10.1116/1.577385

[31] Aanesland, A., and Charles, C., "Plasma Expansion from a Dielectric Electron Cyclotron Resonance Source," *Physica Scripta*, Vol. T122, 2006, pp. 19–24. doi:10.1088/0031-8949/2006/T122/006

[32] Meige, A., Boswell, R. W., Charles, C., and Turner, M. M., "One-Dimensional Particle-in-Cell Simulation of a Current-Free Double Layer in an Expanding Plasma," *Physics of Plasmas*, Vol. 12, No. 052317, 2005, pp. 1–10. doi:10.1063/1.1897390

[33] Sun, X., Cohen, S. A., Scime, E. E., and Miah, M., "On-Axis Parallel Ion Speeds Near Mechanical and Magnetic Apertures in a Helicon Plasma Device," *Physics of Plasmas*, Vol. 12, No. 103509, 2005, pp. 1–8. doi:10.1063/1.2121347

[34] Arefiev, A. V., and Breizman, B. N., "Magnetohydrodynamic Scenario of Plasma Detachment in a Magnetic Nozzle," *Physics of Plasmas*, Vol. 12, No. 043504, 2005, pp. 1–10. doi:10.1063/1.1875632

[35] Charles, C., and Boswell, R. W., "Time Development of a Current-Free Double-Layer," *Physics of Plasmas*, Vol. 11, No. 8, Aug. 2004, pp. 3808–3812. doi:10.1063/1.1764829

A. Gallimore
Associate Editor